Distinguishing between Structural Models of β′-sialons using a Combined Solid-State NMR, Powder XRD and Computational Approach

V. R. Seymour[1,2] and M. E. Smith[1,3]

1. Department of Chemistry, Lancaster University, Bailrigg, Lancaster, LA1 4YB, UK

2. Materials Science Institute, Lancaster University, Bailrigg, Lancaster, LA1 4YB, UK

3. Vice-Chancellor's Office, University House, Lancaster University, Bailrigg, Lancaster, LA1 4YW, UK.

Supporting Information

S1. Structural parameters from diffraction and models for β'-sialons in the literature

A structure for the parent β-Si_3N_4[1] and structures for $Si_{6-z}Al_zO_zN_{8-z}$ (z = 1, 2, and 4) were obtained from the literature.[2,3] The unit cell parameters are given in Table S1 and the unit cells for the β'-sialons are shown in Figure S1. These show the limitation of the diffraction methods used, where the site occupancy of the Al/Si and N/O atoms is averaged over the unit cell. The model β'-sialon structures of this work were based on the β-Si_3N_4 unit cell of Ref. 1. The models are named in reference to their Al/O distribution, and the composition of parent unit cells used to create the supercell required to accommodate the distribution. Domain 113 and Domain 116 are domain models with supercells of 1 x 1 x 3 and 1 x 1 x 6, respectively; Plane 221 is a plane model with a supercell of 2 x 2 x 1; Channel 231 and Channel 331 are channel models with supercells of 2 x 3 x 1 and 3 x 3 x 1, respectively. The models are shown in Figure S2, and the definition of a layer for the domain models is shown in Figure S3.

	Expt. parameters		Unit cell lengths (Å)		Angles (°)		Volume (Å^3)	Ref (ICSD Code)	% difference from β-Si_3N_4		
Z	Temp. T	Type X/N	a	c	α	γ	V		a	c	V
0	RT	X	7.5950	2.9023	90	120	144.986794	Ref. 1 (8263)			
1	RT	N	7.6072	2.9274	90	120	146.710907	Ref. 2 (39496)	0.16	0.86	1.19
2	4.2 K	N	7.6430	2.9450	90	120	148.985380	Ref. 3 (34288)	0.63	1.47	2.76
4	4.2 K	N	7.6920	2.9900	90	120	153.207619	Ref. 3 (34287)	1.28	3.02	5.67
2	300 K	N	7.649	2.950	90	120	149.472740	Ref. 3	0.71	1.64	3.09
4	300 K	N	7.695	2.995	90	120	153.583553	Ref. 3	1.32	3.19	5.93

Table S1: Experimental unit cell parameters taken from the literature for β'-sialon structures.
(X = X-ray diffraction data, N = Neutron diffraction data)

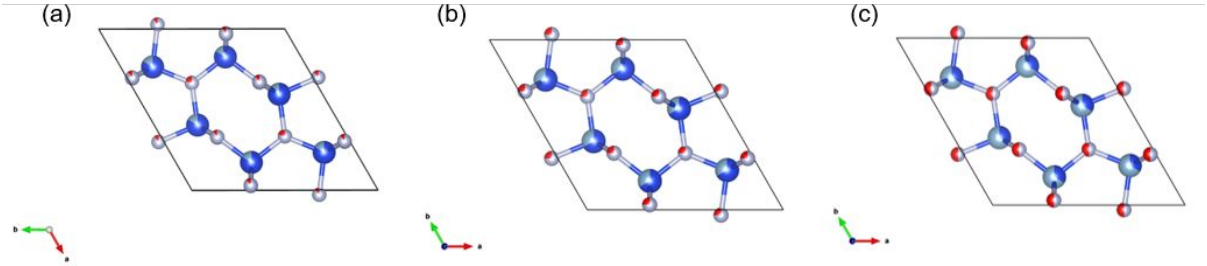

Figure S1: Crystal structures of β'-sialons shown as unit cells with atoms (Al (light blue), Si (blue), O (red) and N (grey)) depicted as pie charts indicating site occupancy, averaged over the structure, (a) z = 1,[2] (b) z = 2 and (c) z = 4.[3] Unit cell figures were created using VESTA.[4]

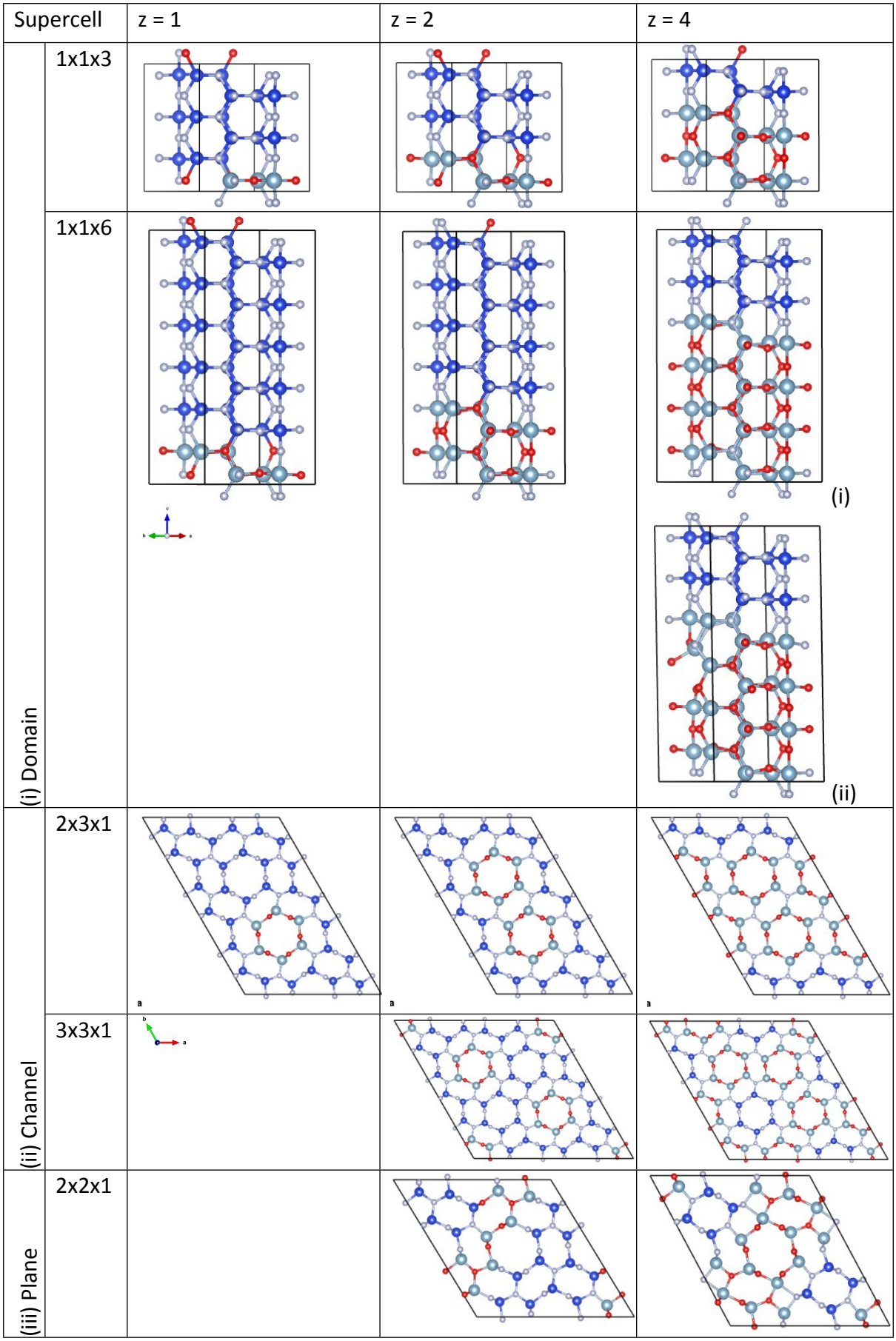

Figure S2: Unit cells of β'-sialon models, showing distribution of Al (light blue), Si (blue), O (red) and N (grey).

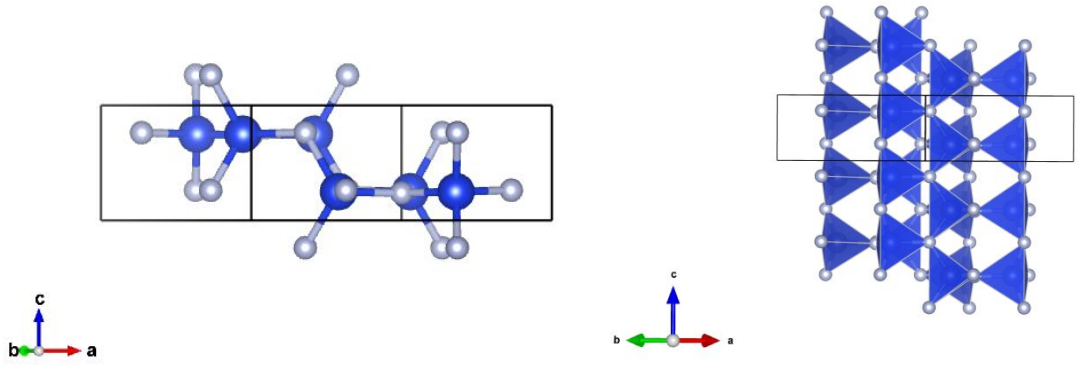

Figure S3: Unit cell of β-Si_3N_4, showing the definition of a layer for the domain models. Layer = one unit cell of β-Si_3N_4 (which contains Si_6N_8).

S2. Previously reported solid-state NMR observations from β'-sialons

	NMR Reference
β-Si_3N_4	^{15}N[5], ^{29}Si[6-8]
β'-, z = 0.05, 0.075, 0.125	^{27}Al[9]
β'-sialon, z = 0.25	^{27}Al[10]
β'-sialon, z = 0.6, 0.9	^{15}N[10], ^{29}Si[10]
β'-sialon, z = 1	^{27}Al[11,12], ^{29}Si[6]
β'-sialon, z = 2	^{27}Al[11,12]
β'-sialon, z = 2.7	^{27}Al[10], ^{29}Si[10]
β'-sialon, z = 4	^{27}Al[11,12], ^{29}Si[6]

Table S2. Summary of references of previous reports of solid-state NMR from β'-sialons.

S3. Powder X-ray diffraction patterns

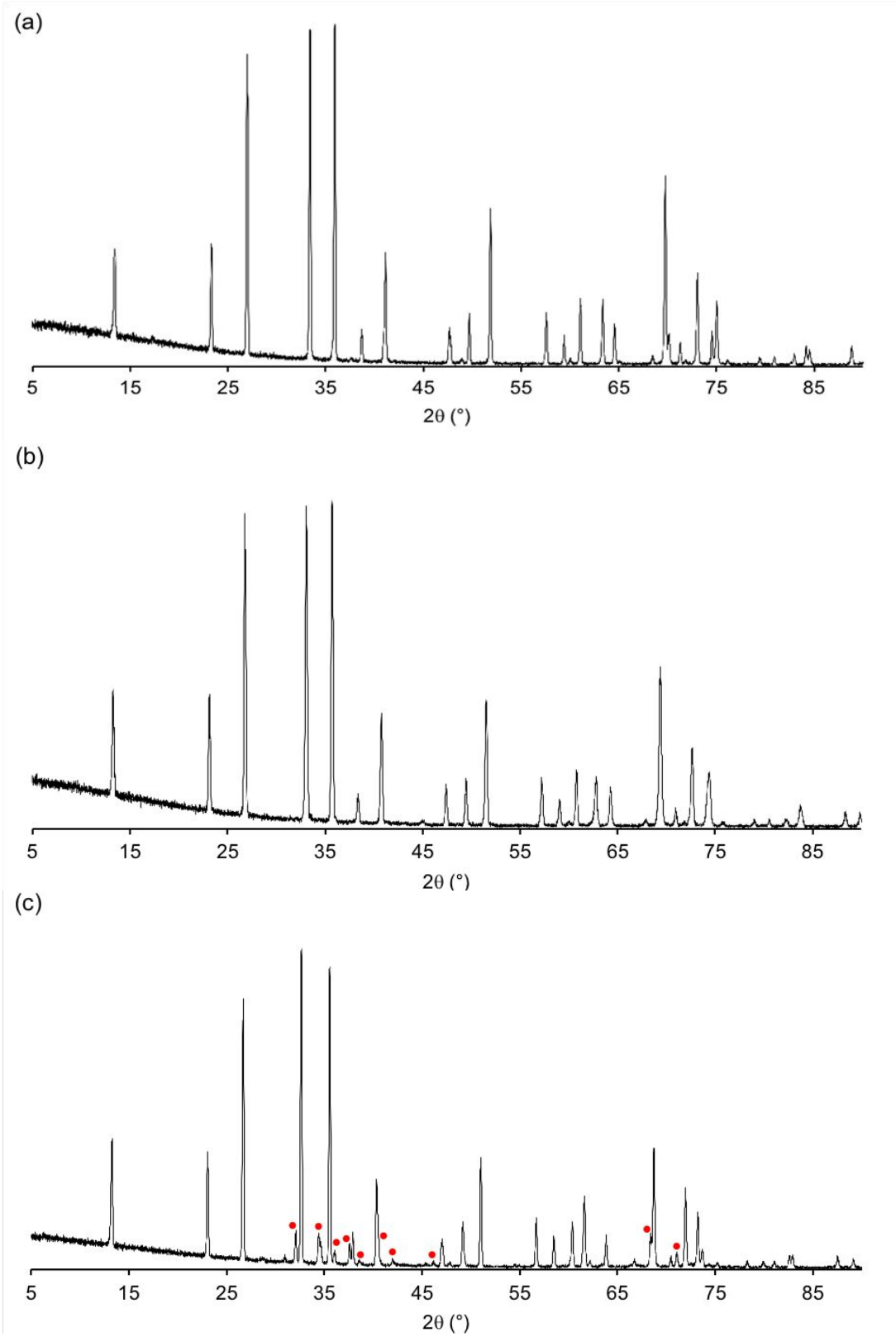

Figure S4: XRD of β'-sialon materials, $Si_{6-z}Al_zO_zN_{8-z}$, (a) z = 1, (b) z = 2, and (c) z = 4. Red dots in (c) indicate impurity peaks. The impurity in the z = 4 sample is identified by XRD and solid-state NMR as 15R polytypoid.

S4. Reference shieldings for DFT (CASTEP) calculations

Reference shielding, σ_{ref}, values were determined using model compounds and comparing calculated NMR parameters to literature NMR parameters.[6,11,13] For ^{27}Al: AlN (wurtzite), Al_2O_3 (corundum), and Al_2SiO_5 (andalusite) were used (ICSD codes: 54697, 73724, and 172725, respectively). For ^{29}Si: SiO_2 (quartz), β-Si_3N_4, α-Si_3N_4, and Al_2SiO_5 (andalusite) were used (ICSD codes: 41412, 8263, 90146, and 73724, respectively). The isotropic chemical shift, δ_{iso}, is obtained from $-(\sigma_{iso} - \sigma_{ref})$.

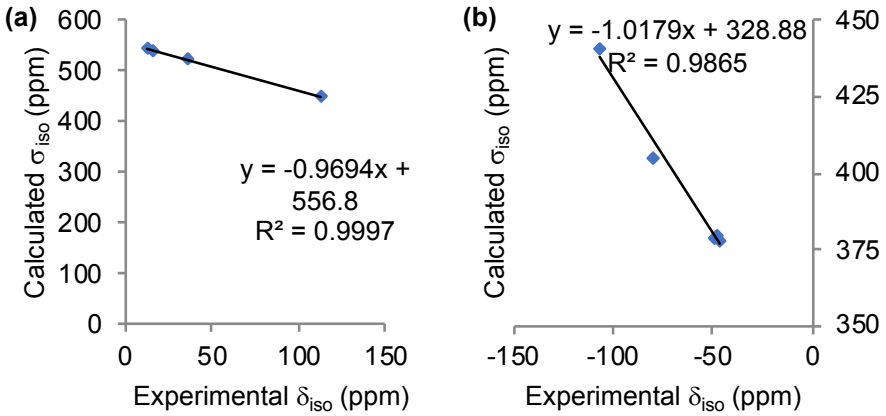

Figure S5: Plot of calculated (CASTEP) σ_{iso} vs experimental (literature) δ_{iso} for a sets of model systems for (a) ^{27}Al and (b) ^{29}Si.

S5. ^{29}Si MAS NMR spectra

The ^{29}Si MAS NMR spectra for the β′-sialons are shown in Figure S6. These show a peak position of approximately −48 ppm.

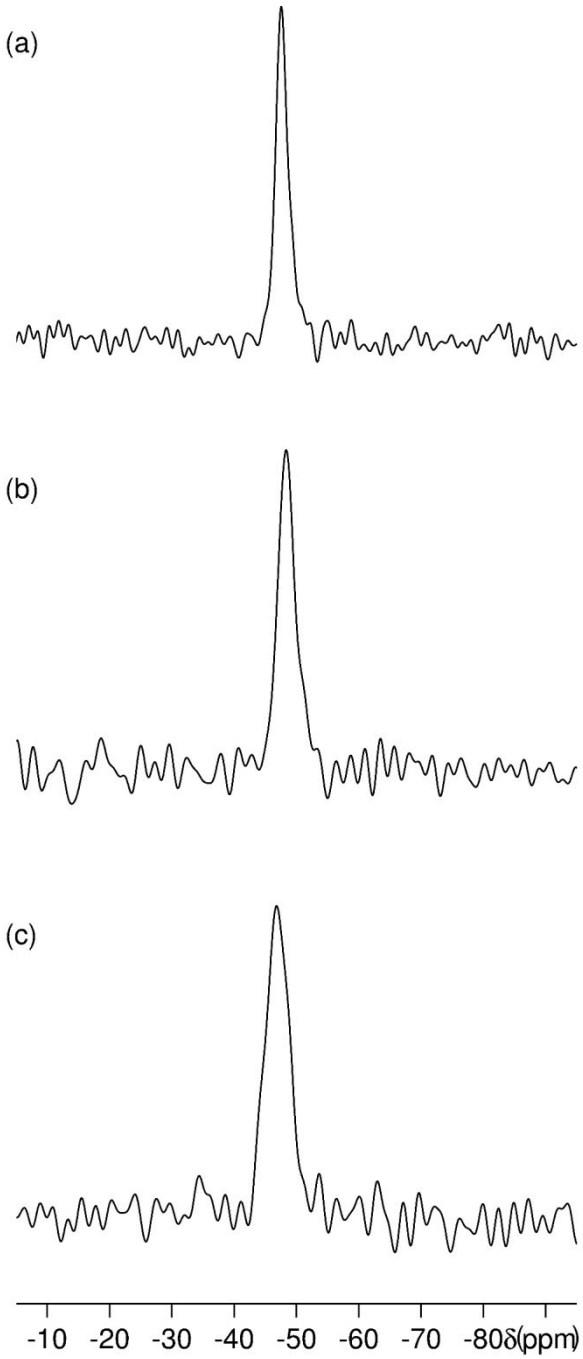

Figure S6: ^{29}Si MAS NMR spectra (16.4 T, 10 kHz MAS) of β′-sialons, (a) z = 1, (b) z = 2, and (c) z = 4.

S6. ^{27}Al MAS NMR spectra, 3Q projections and summary of 1D MAS NMR parameters

^{27}Al MAS NMR spectra and corresponding projections from the ^{27}Al MQMAS spectra are shown in Figure S7.

	16.4 T		20.0 T	
	Peak max. (ppm) (±0.5)	Full width at half max. in ppm, (in Hz) ±1.0/(~100)	Peak max. (ppm) (±0.5)	Full width at half max. in ppm, (in Hz) ±1.0/(~100)
z = 1	72.9	43.3 (7900)	79.3	36.1 (8000)
z = 2	70.1	37.9 (6900)	74.9	30.3 (6700)
z = 4	70.7	31.5 (5750)	77.5	32.0 (7100)

Table S3: Position of peak maxima and full width at half maximum of ^{27}Al MAS NMR spectra.

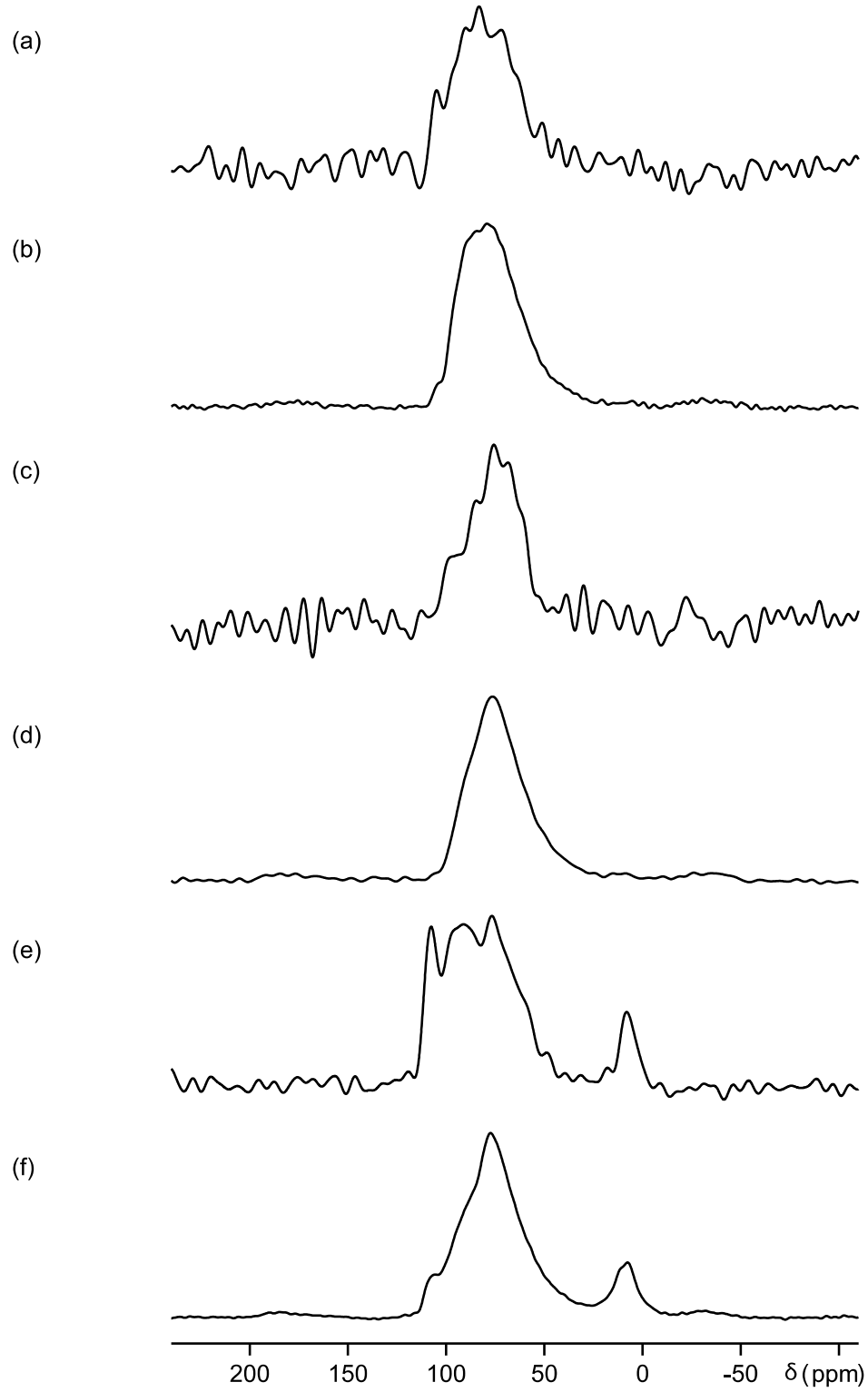

Figure S7: ^{27}Al spectra (20.0 T, 25 kHz MAS) for (a,b) z = 1, (c,d) z = 2, and (e,f) z = 4. (a,c,e) 1D sum projections from MQ MAS spectra and (b,d,f) 1D MAS NMR spectra.

S7 Experimental and calculated cell parameters and volumes as a function of z in β'-sialons

The experimental unit cell parameters were compared to the geometry-optimised model structures. Figure S8 shows the trend in experimental unit cell parameters; the unit cell lengths, and volume, increase across the series as the content of Al/O increases. Figure S9 shows the change in unit cell parameters (as a % difference from the parent β-Si_3N_4) for the geometry-optimised structures of the different models. For z = 4, two domain 116 models were examined (labelled i and ii), with variation at the interface region. As can be seen in Figure S2, the domain 116ii model distorted after geometry optimisation, resulting in an AlO_3N_2 site. The geometry optimisation for this model was rerun using the geometry-optimised domain 116i model as the starting structure, but again a defect structure was obtained. The NMR parameters for the former version of this model are reported in this work. For z = 4, another defect occurred in the geometry-optimised structure of the plane 221 model, AlO_4N.

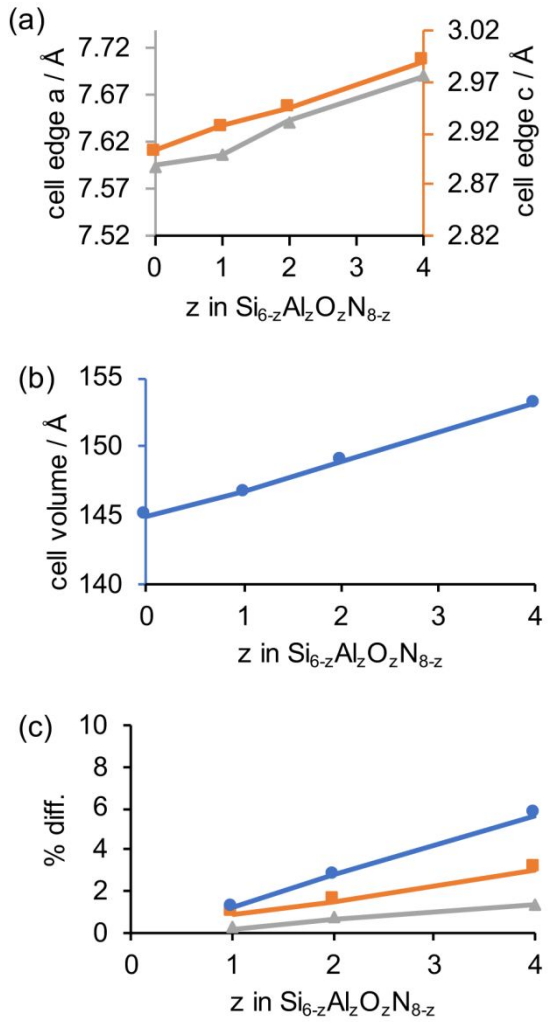

Figure S8: Experimental unit cell information from across the β'-sialon series studied in this work.[1-3] (a) Unit cell lengths, a and c, (b) unit cell volume, and (c) % difference of β'-sialon unit cell parameters compared to the parent β-Si_3N_4. Blue circles: volume; gray triangles: cell length a; orange squares: cell length c.

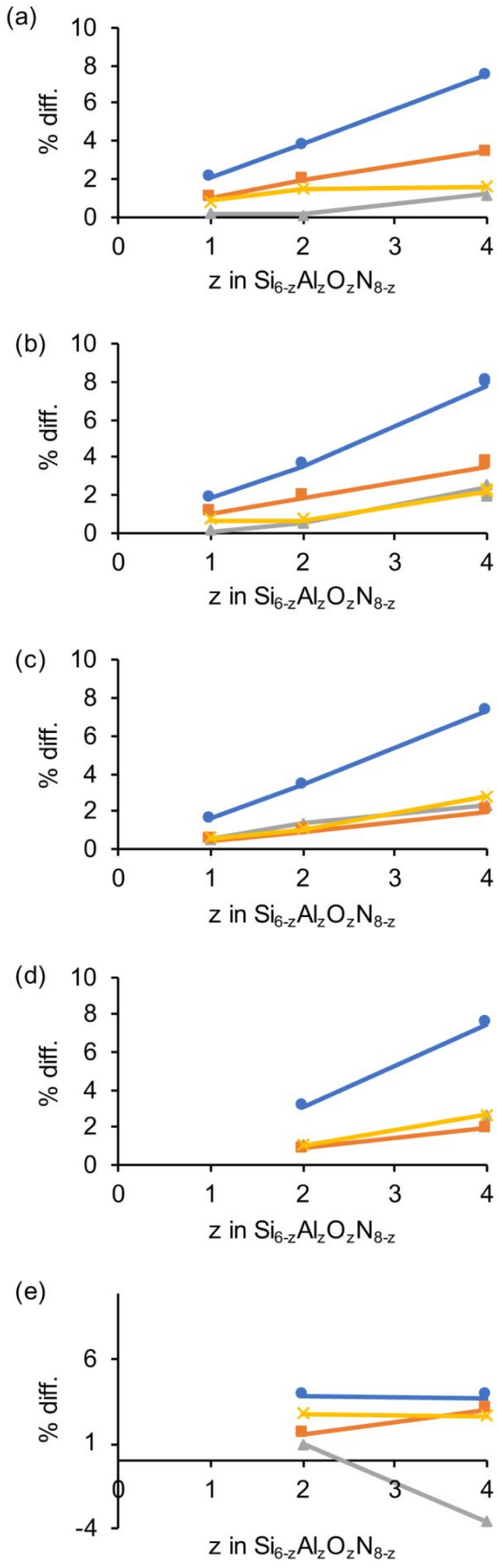

Figure S9: Unit cell (lengths and volume) changes (% compared to parent β-Si_3N_4) for the various models (geometry-optimised structures) used in the computational study; (a) domain 113, (b) domain 116, (c) channel 231, (d) channel 331, (e) plane 221. Blue circles: volume; gray triangles: cell length a; yellow crosses: cell length b; orange squares: cell length c.

S8 Calculated ^{27}Al NMR interaction parameters for each individual model, their positions superimposed on 3Q MAS NMR and simulations of the MAS NMR spectra for possible different layer thicknesses

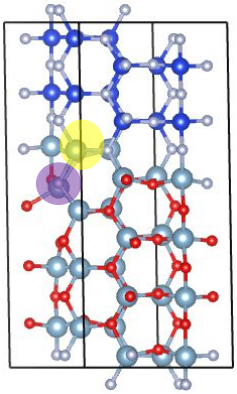

Figure S10: AlN_4 site highlighted in yellow. Defect site highlighted in purple.

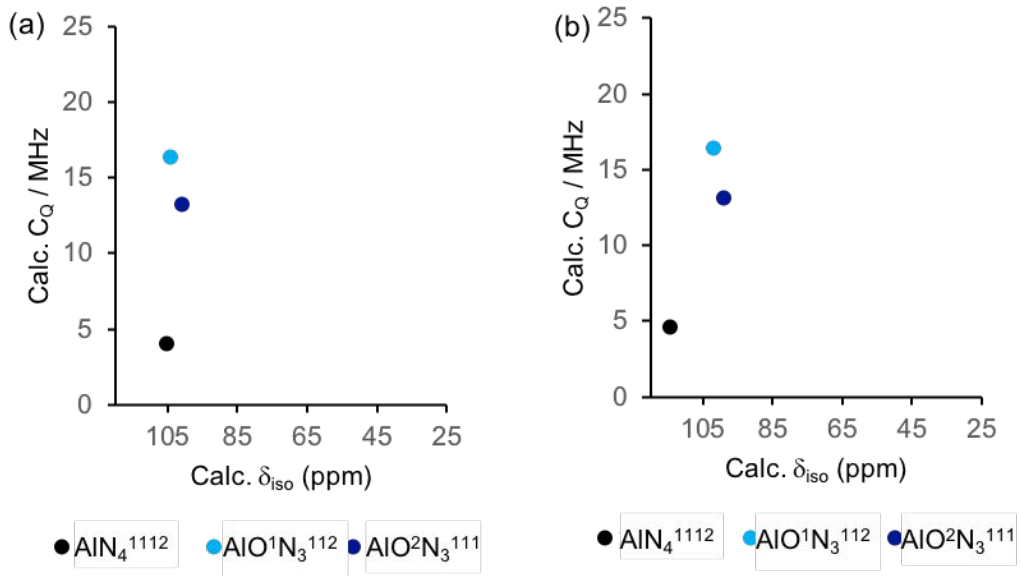

Figure S11: Plot of calculated (CASTEP) ^{27}Al NMR parameters for isolated defects within a 2 x 2 x 2 unit cell of β-Si_3N_4, as studied in Ref. 9, a single Al/O substitution corresponding to β'-sialon with z = 0.125. Geometry optimisation carried out by: (a) atomic coordinates relaxed within a unit cell lattice parameters fixed to those of z = 0.075, following the computational method in Ref. 9, and (b) both atomic coordinates and unit cell allowed to relax, following the method of the present work.

A single Al/O substitution into the 2 x 2 x 2 supercell of β-Si_3N_4 corresponds to β'-sialon with z = 0.125. The calculated ^{27}Al NMR parameters are shown in the plot above. The C_Q values are similar to those reported in the plot in Ref. 9. For an isolated AlN_4 site a C_Q of <5 MHz is obtained. The C_Q calculated for AlN_4 in one of the models for z = 4 is large due to its through bond connectivity to an unintended defect site, obtained after geometry optimisation.

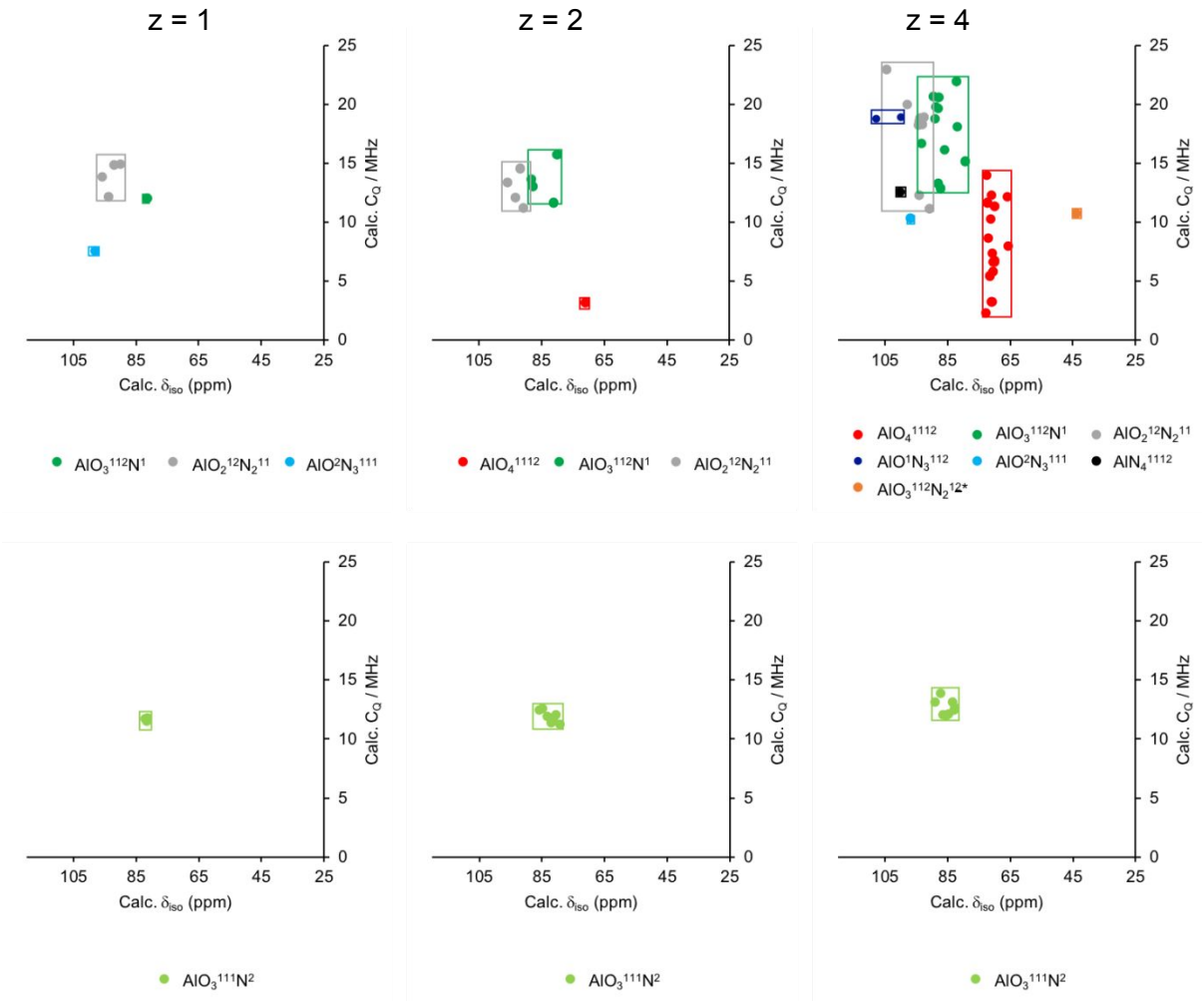

Figure S12: Plot of calculated (CASTEP) ^{27}Al NMR parameters for (top) domain models, and (bottom) channel models, for z = 1, z = 2, and z = 4.

Model	Local Al Environment	Calculated ranges of ^{27}Al C_Q / MHz
z = 1		
Channel	$AlO_3^{111}N^2$	11.5 - 11.8
Domain	$AlO^2N_3^{111}$	7.6
	$AlO_2^{12}N_2^{11}$	12.2 - 14.9
	$AlO_3^{112}N^1$	12.0
z = 2		
Channel	$AlO_3^{111}N^2$	11.2 - 12.6
Domain	$AlO_2^{12}N_2^{11}$	11.2 - 14.6
	$AlO_3^{112}N^1$	11.6 - 15.7
	AlO_4^{1112}	3.2
z = 4		
Channel	$AlO_3^{111}N^2$	12.0 - 13.9
Domain	AlN_4^{1112}	12.6
	$AlO^1N_3^{112}$	18.7 - 18.9
	$AlO^2N_3^{111}$	10.4
	$AlO_2^{12}N_2^{11}$	11.1 - 22.9
	$AlO_3^{112}N^1$	12.9 - 22.0
	AlO_4^{1112}	2.3 - 14
	$AlO_3^{112}N_2^{12}$*	10.8

Table S4: Calculated ranges of ^{27}Al C_Q values. The AlN_4^{1112} site, from model domain116ii, is connected, via N^2 to the $AlO_3^{112}N_2^{12}$*defect site after geometry optimisation (Figure S10), resulting in the large C_Q.

z = 1

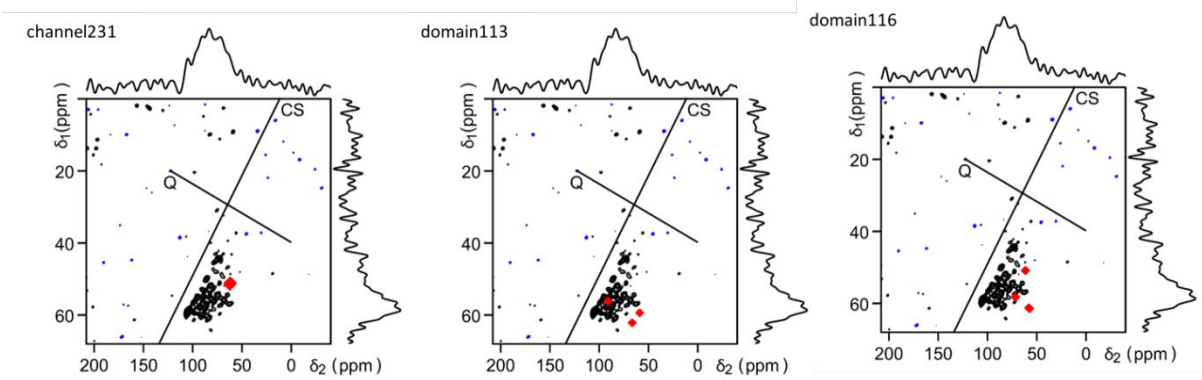

z = 2

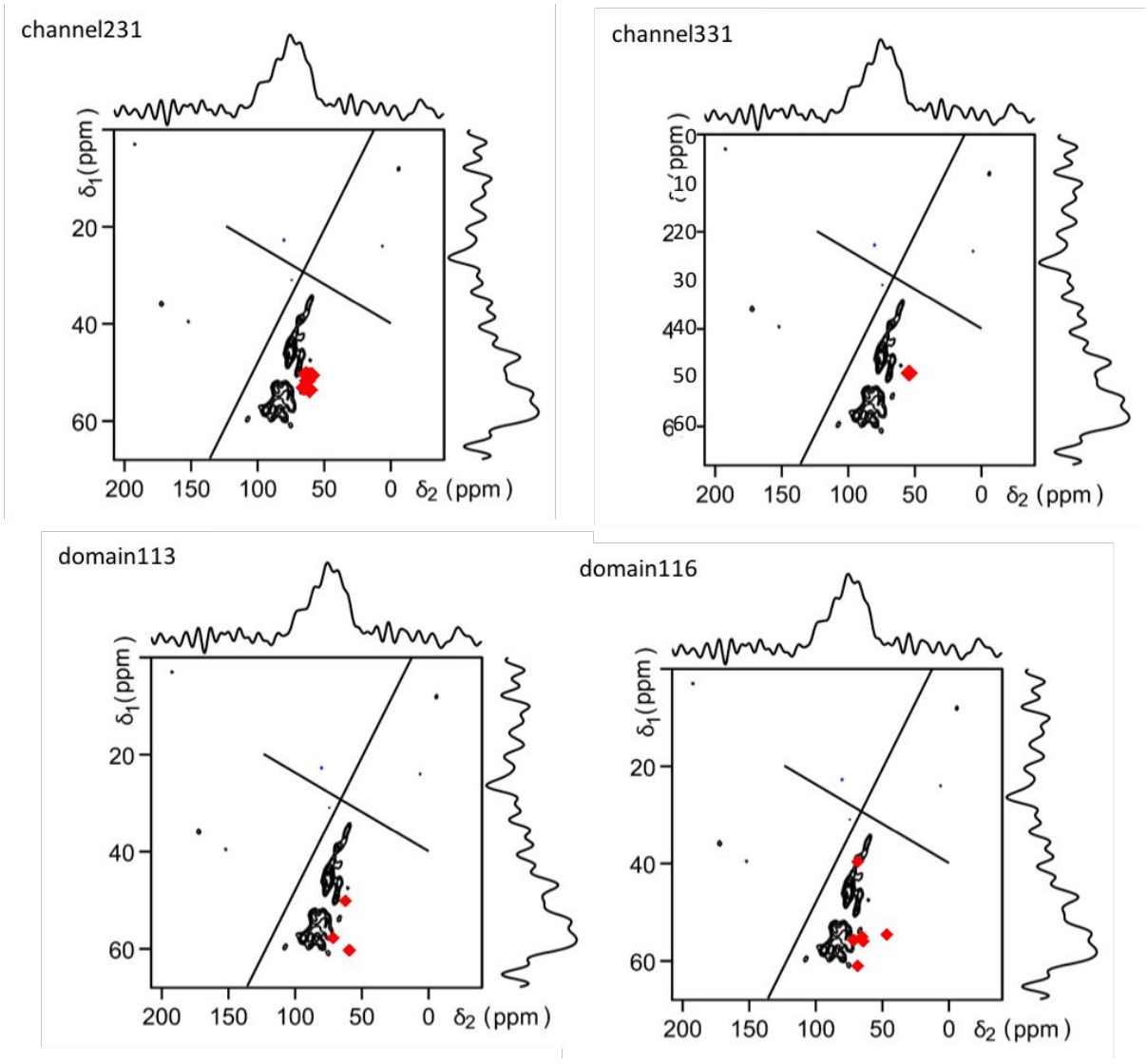

Figure S13: Comparison of 3Q MAS NMR data (20.0 T) with the expected position of the intensity for z = 1 and z = 2 β′-sialons for different structural models. Red diamonds = MQMAS centre-of-gravity of CASTEP calculated ^{27}Al NMR parameters. Spread of data supports single layer thickness for z = 1 (domain 116 model).

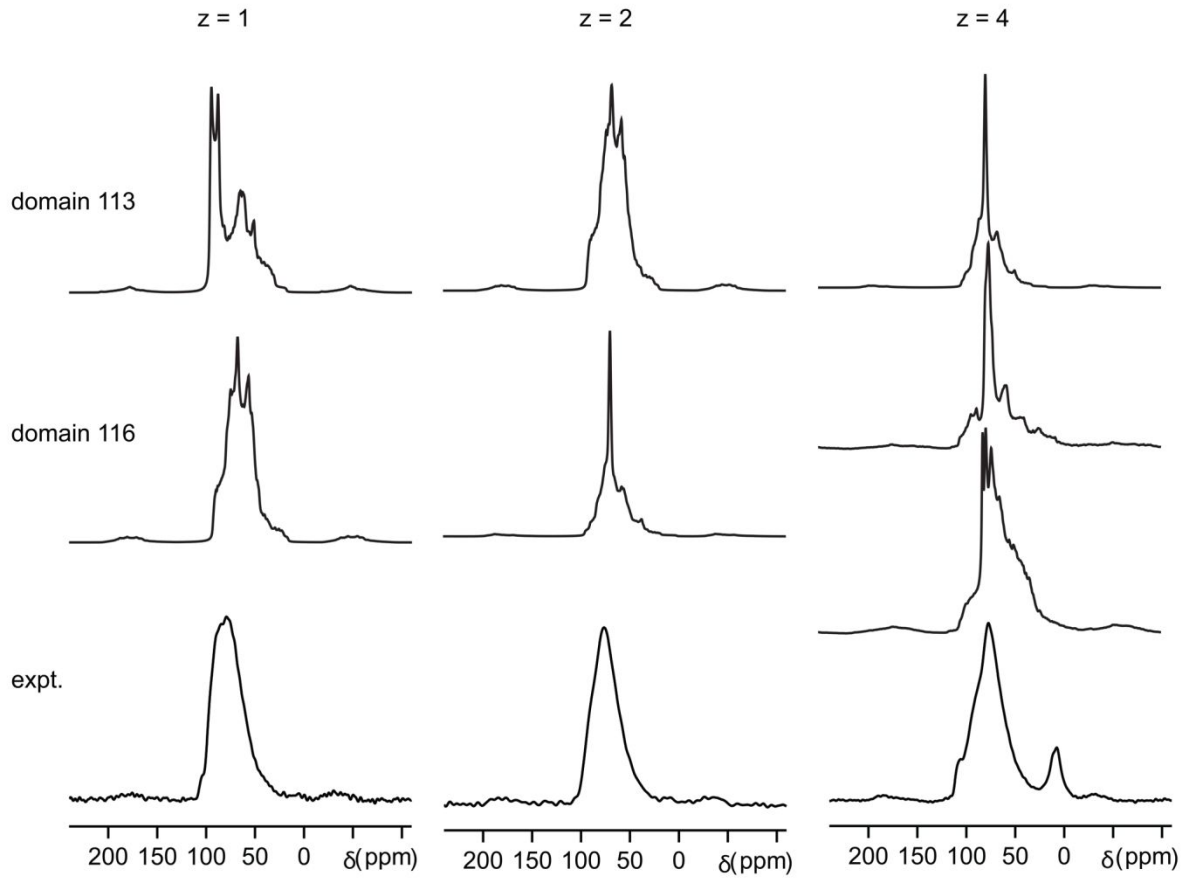

Figure S14: Experimental and simulated spectra (20.0 T, 25 kHz MAS) for z = 1, 2, and 4. Spectra were simulated using SIMPSON, using the NMR parameters calculated by CASTEP for the domain models. The two domain 116 models correspond to those shown in Figure S2.

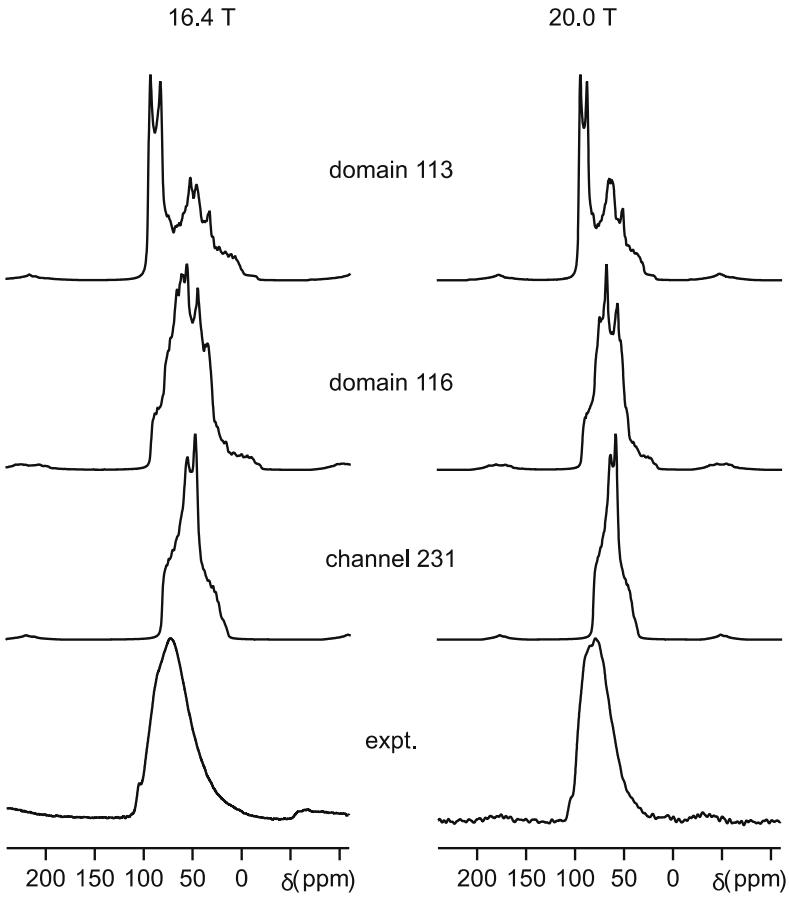

Figure S15: Experimental and simulated spectra (16.4 T, 30 kHz MAS; 20.0 T, 25 kHz MAS) for z = 1. Spectra were simulated using SIMPSON, using the NMR parameters calculated by CASTEP for the domain and channel models.

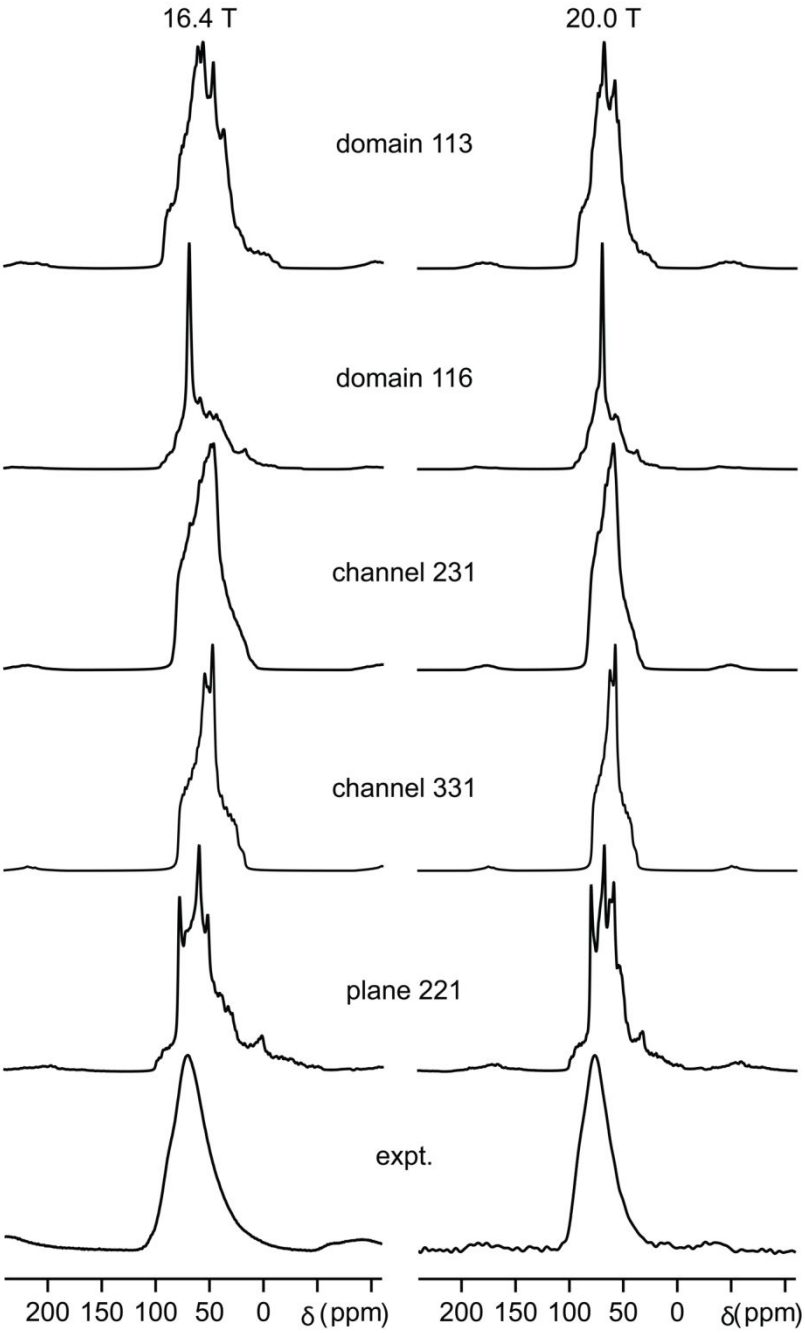

Figure S16: Experimental and simulated spectra (16.4 T, 30 kHz MAS; 20.0 T, 25 kHz MAS) for z = 2. Spectra were simulated using SIMPSON, using the NMR parameters calculated by CASTEP for the domain, channel and plane models.

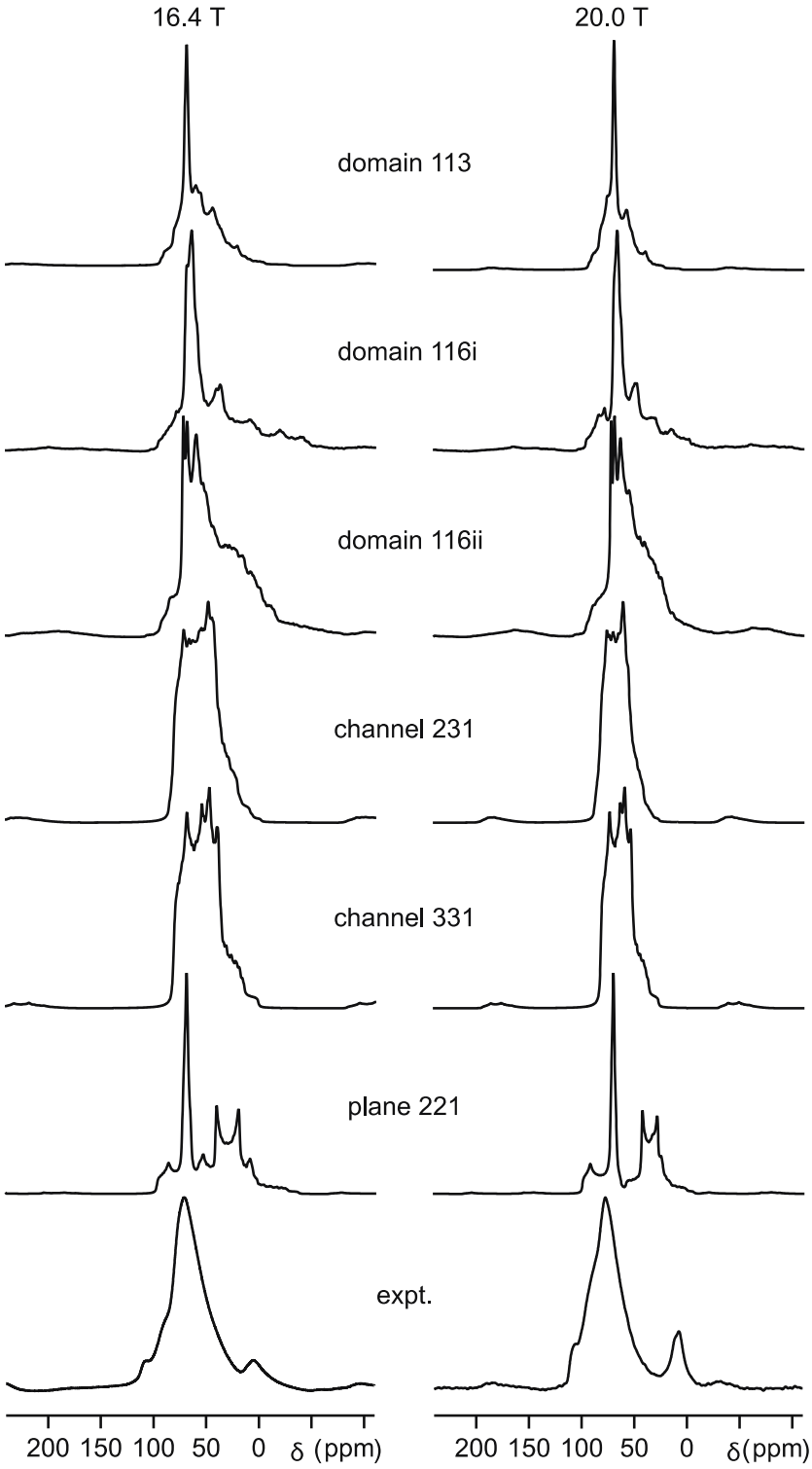

Figure S17: Experimental and simulated spectra (16.4 T, 30 kHz MAS; 20.0 T, 25 kHz MAS) for z = 4. Spectra were simulated using SIMPSON, using the NMR parameters calculated by CASTEP for the domain, channel and plane models.

S9. Example SIMPSON input files

SIMPSON simulations (SIMPSON version 4.2.1)[14] were carried out for the CASTEP-calculated NMR parameters (chemical shift and quadrupolar parameters, C_Q and η_Q) for each of the models. Example SIMPSON input files are given below. The first is for the channel model of z = 1 at 16.4 T with 30 kHz MAS (z1_channel231_700_30.in), and the second is for a domain model of z = 1 at 20.0 T with 25 kHz MAS (z1_domain116_850_25.in), similar to experimental conditions. The zcw4180 crystal file was used for imitating the powder averaging.

z1_channel231_700_30.in

```
# Efficient simultation of MAS quadrupole and CSA spectrum of several independent
# nuclei.
#
# Initial density operator is Ix, i.e., ideal excitation assumed.
# Only the central transition is 'observed'.
#
# The parameters for each nucleus are set in the 'proc main {} { .. }' section of the input file.
#
# The relative contribution of each nucleus to the spectrum is specified by the weight parameter.
# The relative orientation of the CSA and quadrupole coupling tensors is specified by taking the
# quadrupole tensor as coincident with the crystal frame and only specifying the chemical shift tensor orientation.

spinsys {
  channels 27Al
  nuclei   27Al
  shift     1  $par(CSiso) $par(CSaniso) $par(CSeta) $par(alpha) $par(beta) $par(gamma)
  quadrupole 1  2          $par(CQ)     $par(etaQ)  0  0        0
}

par {
  start_operator   I1x
  detect_operator  I1c
  spin_rate       30000
  gamma_angles    40
  sw              300000
  crystal_file    zcw4180
  np              1024
  proton_frequency 700e6
  verbose         111

  variable        tdwell    1.0e6/sw
}

proc pulseq {} {
  global par

  reset
  acq
  for {set i 1} {$i < $par(np)} {incr i} {
      delay $par(tdwell)
      acq
     }
}

proc main {} {
  global par


#  create a dataset of zeros
  set f [fcreate -np $par(np) -sw $par(sw)]

#                C_Q   eta_Q  CSiso  CSaniso CSeta  a  b  g  weight
  foreach Spin_pars {{11.51e6 0.7 14913.816 0 0 0 0 0 2}
{11.76e6 0.72 14853.61344 0 0 0 0 0 2}
{11.71e6 0.74 15001.38336 0 0 0 0 0 2}} {
# Note the position of the brackets at the end of the above line.  There must be a single
# space between two braces otherwise the foreach command doesn't work. Strange!
#
  set par(CQ)      [lindex $Spin_pars 0]
  set par(etaQ)    [lindex $Spin_pars 1]
  set par(CSiso)   [lindex $Spin_pars 2]
  set par(CSaniso) [lindex $Spin_pars 3]
  set par(CSeta)   [lindex $Spin_pars 4]
  set par(alpha)   [lindex $Spin_pars 5]
  set par(beta)    [lindex $Spin_pars 6]
  set par(gamma)   [lindex $Spin_pars 7]
  set par(weight)  [lindex $Spin_pars 8]

#  run the simulation for each site
  set  g         [fsimpson]

#  weight each site as required
  fexpr $g $par(weight)*\$re $par(weight)*\$im

#  add the sites together
  fadd  $f $g
 }

  fsave $f $par(name).fid
  fzerofill $f 8192
  faddlb $f 300 0
  fft $f
  fsave $f $par(name).spe
}
```

z1_domain116_850_25.in

```
# Efficient simultation of MAS quadrupole and CSA spectrum of several independent
# nuclei.
#
# Initial density operator is Ix, i.e., ideal excitation assumed.
# Only the central transition is 'observed'.
#
# The parameters for each nucleus are set in the 'proc main {} { .. }' section of the input file.
#
# The relative contribution of each nucleus to the spectrum is specified by the weight parameter.
# The relative orientation of the CSA and quadrupole coupling tensors is specified by taking the
# quadrupole tensor as coincident with the crystal frame and only specifying the chemical shift tensor orientation.

spinsys {
  channels 27Al
  nuclei   27Al
  shift     1  $par(CSiso) $par(CSaniso) $par(CSeta) $par(alpha) $par(beta) $par(gamma)
  quadrupole 1  2          $par(CQ)     $par(etaQ)  0  0        0
}

par {
  start_operator   I1x
  detect_operator  I1c
  spin_rate       25000
  gamma_angles    40
  sw              300000
  crystal_file    zcw4180
  np              1024
  proton_frequency 850e6
  verbose         111

  variable        tdwell    1.0e6/sw
}

proc pulseq {} {
  global par

  reset
  acq
  for {set i 1} {$i < $par(np)} {incr i} {
     delay $par(tdwell)
     acq
     }
}

proc main {} {
  global par


#  create a dataset of zeros
  set f [fcreate -np $par(np) -sw $par(sw)]

#                C_Q   eta_Q  CSiso  CSaniso CSeta  a  b  g  weight
  foreach Spin_pars {{14.88e6 0.85 20406.14604 0 0 0 0 0 1}
{12.00e6 0.48 18042.55965 0 0 0 0 0 1}
{12.19e6 0.7 20758.35807 0 0 0 0 0 1}
{14.88e6 0.86 20401.7157 0 0 0 0 0 1}
{12.00e6 0.48 18046.98999 0 0 0 0 0 1}
{12.18e6 0.69 20760.57324 0 0 0 0 0 1}} {
# Note the position of the brackets at the end of the above line.  There must be a single
# space between two braces otherwise the foreach command doesn't work. Strange!
#
  set par(CQ)      [lindex $Spin_pars 0]
  set par(etaQ)    [lindex $Spin_pars 1]
  set par(CSiso)   [lindex $Spin_pars 2]
  set par(CSaniso) [lindex $Spin_pars 3]
  set par(CSeta)   [lindex $Spin_pars 4]
  set par(alpha)   [lindex $Spin_pars 5]
  set par(beta)    [lindex $Spin_pars 6]
  set par(gamma)   [lindex $Spin_pars 7]
  set par(weight)  [lindex $Spin_pars 8]

#  run the simulation for each site
  set  g         [fsimpson]

#  weight each site as required
  fexpr $g $par(weight)*\$re $par(weight)*\$im

#  add the sites together
  fadd  $f $g
 }

  fsave $f $par(name).fid
  fzerofill $f 8192
  faddlb $f 300 0
  fft $f
  fsave $f $par(name).spe
}
```

S10. References

[1] Gruen, R. The crystal structure of beta-Si_3N_4; structural and stability considerations between alpha- and beta-Si_3N_4. *Acta Crystallographica, Section B: Structural Crystallography and Crystal Chemistry* **1979**, *35*, 800-804.

[2] Khvatinskaya, D.Y.; Em, VV.T.; Loryan, E.; Smirnov, K.L. A neutron diffraction study on the structure of β'-sialon. *Inorg. Mater.* **1991**, *27*, 1805-1807.

[3] Gillott, L.; Cowlam, N.; Bacon,G.E. A neutron diffraction investigation of some β'-sialons, *J. Mater. Sci.* **1981**, *16*, 2263-2268.

[4] Momma, K.; Izumi, F. VESTA 3 for three-dimensional visualization of crystal, volumetric and morphology data. *J. Appl. Crystallogr.,* **2011**, *44*, 1272-1276.

[5] Harris, R.K.; Leach, M.J.; Thompson D.P. Synthesis and magic-angle spinning nuclear magnetic resonance of ^{15}N-enriched silicon nitrides. *Chem. Mater.* **1990**, *3*, 320-323.

[6] Dupree, R.; Lewis, M.H.; Leng-Ward, G.; Williams, D.S. Coordination of Si atoms in silicon-oxynitrides determined by magic-angle-spinning NMR. *J. Mater. Sci. Lett.* **1985**, *4*, 393-395.

[7] Carduner, K.R.; Carter, R.O.; Millberg M.E.; Crosbie, G.M. Determination of phase-composition of silicon-nitride powders by ^{29}Si magic angle spinning nuclear-magnetic-resonance spectroscopy. *Anal. Chem.* **1987**, *59*, 2794-2797.

[8] Carduner, K.R.; Blackwell, C.S.; Hammond, W.B.; Reidinger, F.; Hatfield, G.R. ^{29}Si NMR characterization of α-silicon and β-silicon nitride. *J. Am. Chem. Soc.* **1990**, *112*, 4676-4679.

[9] Cozzan, C.; Griffith, K.J.; Laurita, G.; Hu, J.G.; Grey, C.P.; Seshadri, R. Structural Evolution and Atom Clustering in β-SiAlON: β-$Si_{6-z}Al_zO_zN_{8-z}$ *Inorg. Chem*. **2017**, *56*, 2153-2158.

[10] Sjöberg, J.; Harris R.K.; Apperley D.C. ^{29}Si, ^{27}Al and ^{15}N magic-angle spinning nuclear magnetic resonance of O'-sialons and some related phases. *J. Mater. Chem.* **1992**, *2*, 433-438.

[11] Dupree, R.; Lewis M.H.; Smith, M.E. Structural characterization of ceramic phases with high-resolution ^{27}Al NMR. *J. Appl. Cryst*. **1988**, *21*, 109-116.

[12] Smith, M.E. Observation of mixed $Al(O,N)_4$ structural units by ^{27}Al magic angle spinning NMR. *J. Phys. Chem.* **1992**, *96*, 1444-1448.

[13] (a) Rocha, J. Direct observation of highly distorted hexa-coordinated aluminium in andalusite by very fast Al-27 MAS NMR. *Chem. Commun.* **1998**, 2489-2490. (b) . Harris, R.K.; Leach, M.J.; Thompson, D.P. Synthesis and magic-angle-spinning nuclear-magnetic resonance of ^{15}N-enriched silicon nitrides. *Chem. Mater.* **1990**, *2*, 320-323. (c) Jakobsen, H.J.; Skibsted, J.; Bildsøe, H.; Nielsen, N.C. Magic-angle spinning NMR spectra of satellite transitions for quadrupolar nuclei in solids. *J. Magn. Reson.* **1989**, *85*, 173-180. (d) Smith, J.V.; Blackwell, C.S. Nuclear magnetic resonance of silica polymorphs. *Nature* **1983**, *303*, 223-225. (e) Profeta, M.; Mauri,F.; Pickard, C.J. Accurate first principles prediction of O-17 NMR parameters in SiO_2: Assignment of the zeolite ferrierite spectrum. *J. Am. Chem. Soc.* **2003**, *125*, 541-548.

[14] Bak, M.; Rasmussen, J.T.; Nielsen, N.C. SIMPSON: A General Simulation Program for Solid-State NMR Spectroscopy, *J. Magn. Reson.*, **2000**, *147*, 296.